lock fault, but no such explanation can be invoked for TPK. Scatter in these control data indicates that the lateral P-velocity gradient may extend only a few (~ 2) kilometers rather than the 20-km upper limit suggested by the data from locations near major faults. If boreholes GAR and STC are discarded from Fig. 2 on the assumption that they are possibly within the fault zone proper, the significance of the low velocities at LMT, SPH, LHG, GAB, and GBS with respect to the high velocities at FPK and CBL is not compelling evidence that a lateral velocity gradient exists over the 20-km range from the faults. Even if this zone of fractured rock extends only 2 km (rather than 20 km) beyond the mapped active trace and gouge zones of the San Andreas and Garlock faults, it is a significant, and seldom reckoned with, component of our major faults.

A major structure such as the fault-controlled band of fractured rock that we postulate from our V_p studies, extending 2 to 20 km from major faults, has profound implications for earthquake prediction research and other crustal studies conducted in this zone. The lateral fracture gradient that we infer from our V_p gradient may control the decrease in shear stress reported by Zoback and Roller (*12*) approaching the San Andreas fault near Palmdale (Fig. 2). The similarity between the V_p and stress curves (Fig. 2) suggests some relation between V_p and stress. The increase in maximum horizontal stress (σ_1) with distance from the fault may increase V_p by holding closed more cracks and fractures (*13*). On the other hand, increased fracturing nearer the fault may allow this zone to adjust more easily to stress changes, placing a limit on the amount of strain near-surface rocks may accumulate before the fractures accommodate the stress. Chan *et al.* (*14*) attribute large discrepancies between observed and predicted strains (and the inferred stresses) during heating experiments in hard granite to expansion of the rock into preexisting fractures. Similar adjustments probably occur in fractured rock as tectonic stress gradually increases.

Many experiments conducted in search of earthquake precursors are located within 10 km of major faults, possibly within this zone of fractured rock. Strain and tilt, changes in ground-water levels or radon emission rates, anomalies in electrical measurements or seismic wave propagation, and perhaps other phenomena reported as possible earthquake precursors should be sensitive to changes in these fractures as the crust responds to a changing strain field. Lateral rigidity gradients and anisotropy in these fractured rocks contribute additional complexity. If dilatancy occurs prior to earthquakes, it is probably confined to fractures adjacent to the fault rather than distributed through the more competent crustal rocks at greater distances. We must, at the very least, unravel the seismic velocity structure of fault zones if we are to properly monitor and interpret velocity variations prior to earthquakes. On a broader scale, geophysical measurements near major faults should probably be interpreted in terms of the physical properties of fractured rocks rather than the properties of laboratory samples.

DONALD J. STIERMAN
STEVE O. ZAPPE*
Institute of Geophysics and Planetary Physics, University of California, Riverside 92521

References and Notes

1. D. J. Stierman *et al.*, *Eos* **57**, 961 (1976).
2. D. Moos and M. Zoback, *ibid.* **60**, 939 (1979).
3. R. L. Wesson, J. C. Roller, W. H. K. Lee, *Bull. Seismol. Soc. Am.* **63**, 1447 (1973); D. Hadley and H. Kanamori, *Geol. Soc. Am. Bull.* **88**, 1469 (1977).
4. D. J. Stierman, J. H. Healy, R. L. Kovach, *Bull. Seismol. Soc. Am.* **69**, 397 (1979).
5. J. H. Sass *et al.*, *U.S. Geol. Surv. Open-File Rep. 78-756* (1978).
6. R. E. Warrick, *Bull. Seismol. Soc. Am.* **64**, 375 (1974).
7. S. O. Zappe, thesis, University of California, Riverside (1979).
8. D. J. Stierman and R. L. Kovach, *J. Geophys. Res.* **84**, 672 (1979).
9. M. D. Zoback, S. Hickman, D. Moos, *Eos* **61**, 1032 (1980).
10. B. Sjøgren, A. Øfsthus, J. Sandberg, *Geophys. Prospect.* **27**, 409 (1979).
11. H. Kanamori and D. Hadley, *Pure Appl. Geophys.* **113**, 257 (1975).
12. M. D. Zoback and J. C. Roller, *Science* **206**, 445 (1979).
13. M. Zoback, personal communication.
14. T. Chan, M. Hood, M. Board, paper presented at the American Society of Mechanical Engineers Energy Technology Conference, New Orleans, La., February 1980.
15. J. E. Gibbs, T. E. Fumal, R. D. Borcherdt, *U.S. Geol. Surv. Open-File Rep. 75-564* (1975), p. 67; *U.S. Geol. Surv. Open-File Rep. 76-731* (1976), p. 118.
16. M. D. Zoback, H. Tsukahara, S. Hickman, *J. Geophys. Res.* **85**, 6157 (1980).
17. We thank J. H. Sass of the USGS for the boreholes, D. Moos for unpublished data, and J. H. Healy and M. D. Zoback for stimulation. This work was supported by the Agricultural Experiment Station and intramural grants from the Academic Senate, University of California at Riverside, and by grant EAR 7926331 from the National Science Foundation. D.J.S. is also at the Agricultural Experiment Station, University of California, Riverside.
* Present address: Shell Development Company, Post Office Box 60775, New Orleans, La. 70160.

17 April 1981

Generation of Stabilized Microbubbles in Seawater

Abstract. *Bubbles of less than 1 micrometer and as large as 13.5 micrometers in diameter, stabilized by an apparent compression of substances sorbed onto their surfaces, were examined to determine their physical and temporal stability. Their ease of formation is related to the qualities of the water in which they are formed. Their presence in the water column must now be considered when interpreting acoustic data gathered to determine marine bubble populations.*

Marine bubble populations inferred from acoustic measurements are sometimes very large, strikingly anomalous, and impossible to interpret in terms of conventional mechanisms explaining bubble formation and loss (*1*, *2*). We believe that these large and relatively persistent populations are due to the presence of stable microbubbles, which are a common feature of the near surface region of the oceans and of many aqueous systems.

There is previous evidence for the existence of stable microbubbles. Degens (*3*) found 1-μm hollow spheres as suspended particles in Lake Kivu, East Africa, and suggested that such spheres might be precursors of primordial cells. He concluded that the spheres result when bubbles, forming deep in the remarkable Lake Kivu waters, become coated with resinous materials that are subsequently stabilized by metal ion complexing.

Minute bubbles stabilized by encapsulation in an organic film have long been invoked to explain low thresholds for ultrasonic cavitation in liquids (*4*). The possibility that stable microbubbles are present in the bloodstream and act as nuclei for the formation of larger bubbles has been suggested to explain decompression sickness in scuba and deep-sea divers (*5*). While small bubbles are certainly favored in energetic terms as nuclei for the formation of larger bubbles, many investigators of the physics of nucleation have assumed that gas nuclei exist only in the crevices of hydrophobic surfaces (*6*, *7*). We now present a photographic record of the formation of stable spherical microbubbles and report their temporal and mechanical stability in samples of natural seawater.

In preparation for each experiment, 2 liters of seawater from the Dalhousie University Aquatron seawater inlet were filtered through preoxidized glass fiber filters (Gelman Sciences, model GFD) and then partially degassed under vacuum. The water was then stirred for 10 hours in a shallow bath maintained at

0036-8075/81/0710-0209$00.50/0 Copyright © 1981 AAAS

22°C. This sequence ensured that equilibration with the atmosphere was approached from undersaturation.

An observation cell with glass internal surfaces was constructed to allow viewing and photomicrography. Before an experiment began, all cell and container surfaces with which seawater made contact were scrupulously cleaned in strong detergent solution or hot chromic acid, rinsed thoroughly with deionized and filtered distilled water, and rinsed a minimum of three times with the seawater sample.

Bubbles with initial sizes of from 40 to 100 μm in diameter were produced by shear at the surface of a sintered glass frit (*8*), transferred to a segregation tube (*9*) filled with the seawater sample, and aged in the tube for a minimum of 15 seconds. Between 200 and 400 of the bubbles were than transferred to the observation cell, which had been filled with the equilibrated seawater. When the bubbles rose into the cell and to the underside of its viewing plate, they were examined with a photomicroscope (Zeiss II) capable of resolving bubbles and particles as small as 0.5 μm in diameter. The temperature throughout each experiment remained at 22°C.

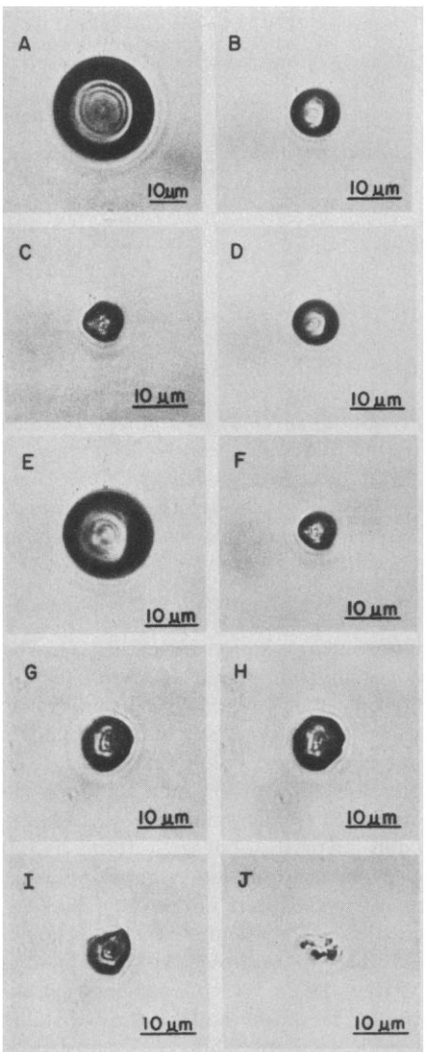

Fig. 1. (A to C) Stable microbubble formed in air-saturated seawater at 22°C and 1 atm. (D and E) Expansion of the microbubble when sufficient negative pressure was applied to the cell contents. (F) Return of the microbubble to nearly its original size and shape when atmospheric pressure was restored. (G) A second microbubble at atmospheric pressure, (H) at 0.28 m of water, and (I) at 0.69 m of water. (J) Particle remaining after collapse of bubble under pressure equivalent to 0.83 m of water.

Once in the cell, all bubbles began to dissolve spontaneously because of their surface tension, and they diminished in size at an increasing rate as dissolution progressed. The dissolution rate became very rapid once the bubbles reached about 10 μm in diameter, and bubbles that dissolved completely did so in less than 10 seconds.

When a bubble dissolved completely, a small transparent particle composed of the material originally present on the bubble at the air-water interface always remained—a familiar result following complete bubble dissolution (*9*). Some bubbles did not dissolve completely, however. They stopped decreasing in size abruptly, sometimes becoming slightly aspherical, and remained as microbubbles apparently stabilized by films compressed during dissolution (Fig. 1, A to C). These microbubbles were readily distinguishable from the transparent particles. The diameters of nearly 800 of these stabilized microbubbles were measured with an ocular micrometer and found to range from less than 1 μm to 13.5 μm. This size range is unexpected because very small bubbles should dissolve rapidly in response to their surface tension pressures, typically about 0.2 atm for a bubble of 13.5 μm, and nearly 3.0 atm for a bubble of 1 μm in diameter. It is obvious that some mechanical or diffusion-limiting effect that resists further bubble dissolution is activated during bubble contraction and the attendant compression of encapsulating surface films.

Small negative and positive changes in pressure could be applied to the contents of the observation cell. When sufficient tension (negative pressure) was applied, the microbubbles expanded (Fig. 1, C to E). Expansion proceeded slowly at first and then more rapidly. When the tension was removed, some bubbles contracted and dissolved completely, but most returned to nearly the same sizes and shapes that they had as stable microbubbles (Fig. 1F).

The application of pressure resulted in rapid and complete dissolution of some of the stable microbubbles (Fig. 1, G to J). In one experiment, a pressure equivalent to 0.83 m of water reduced a population of stable microbubbles by 74 percent. Figure 2A shows size-dependent resistance to pressure apparent in the size distribution of the surviving microbubbles: bubbles 0.75 to 2.25 μm in diameter were reduced in number by slightly more than a factor of 1/3, while those greater than about 5 μm were reduced by a factor of more than 10. A further increase in pressure to 1.38 m of water resulted in the collapse of all remaining visible stabilized microbubbles.

Of the bubbles put into the cell, the percentage that formed stable microbubbles changed little when the experiment was repeated in the same water sample, but varied from 2 to 93 percent in samples taken over the period from 3 to 25 November 1980. In samples taken on 3, 4, and 7 November, stable microbubbles were formed by 24, 25, and 93 percent of the bubbles examined, respectively. However, in two succeeding experiments on 13 and 25 November, the percentage of stable microbubbles fell to only 2 percent. This decrease is most likely due to a change in the concentra-

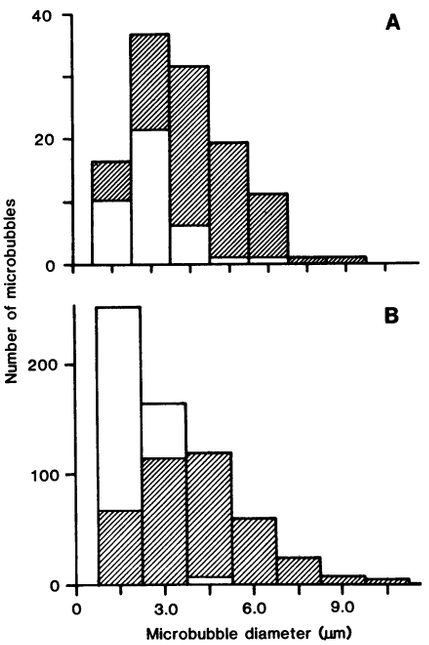

Fig. 2. (A) Distribution pattern (unshaded region) resulting when a population of microbubbles formed in air-saturated seawater at 1 atm and 22°C (shaded region) was subjected to a pressure increase equivalent to 0.83 m of water. Resistance to pressure is inversely related to bubble size. (B) Temporal changes in a population of microbubbles. The original population (shaded region) showed little change in numbers after 22 hours (unshaded region) but did display a marked shift toward smaller size.

tion or character of the natural surfactants in the seawater from Aquatron inlet, a result of increasingly stormy weather and the seasonal decline of biological activity in Labrador Current water over this period. These circumstances strongly suggest a parallel between stable microbubble formation and the seasonal occurrence of natural organic particles (*10*).

In an experiment designed to test microbubble stability as a function of time, a population generated on 7 November was maintained at 22°C in the cell and examined periodically for changes in size and number. After 4 hours there were no apparent changes; after 22 hours, while there was little reduction in number, the microbubbles generally were smaller (Fig. 2B), and bubbles that previously were aspherical had become less so. Thirty hours after formation, few visible microbubbles remained.

Because a significant proportion of the bubbles produced by a breaking wave at sea are smaller than 200 μm in diameter (*11*), and because small bubbles dissolve in saturated seawater as a result of surface tension alone, the number of stable microbubbles that can be produced by breaking waves may be very large and show strong periodicity.

The presence of stabilized microbubbles in various numbers in the marine environment requires investigators of oceanic bubble populations to consider not only the sea state, but the season, the recent history of the sea state, the atmospheric pressure, and other possible bubble sources such as local surf. In particular, bubble populations determined acoustically must be interpreted with regard for the effect of stabilizing surfaces on bubble resonance frequencies. This effect, as Medwin (*12*) points out, can result in an overestimation of bubble size from acoustic data.

While we demonstrated that stable microbubbles do form in seawater, we examined only a relatively small number of such bubbles during a short period. Hence, our data should be considered only as a starting point for continuing study.

BRUCE D. JOHNSON
ROBERT C. COOKE
Department of Oceanography,
Dalhousie University,
Halifax, Nova Scotia, Canada B3H 4J1

References and Notes

1. H. Medwin, *J. Geophys. Res.* **82**, 971 (1977).
2. G. A. Garrettson, *J. Fluid Mech.* **59**, 187 (1973).
3. E. T. Degens, in *The Global Carbon Cycle: SCOPE Report 13*, B. Bolin *et al.*, Eds. (Wiley, New York, 1979), pp. 57–77.
4. F. E. Fox and K. F. Herzfeld, *J. Acoust. Soc. Am.* **26**, 984 (1954).
5. D. E. Yount, Ed., abstracts of papers from the Second Chemical Congress of the North American Continent, Las Vegas, Nev., 1980.
6. E. N. Harvey, D. K. Barnes, W. D. McElroy, A. M. Whiteley, D. C. Pease, K. W. Cooper, *J. Cell. Comp. Physiol.* **24**, 1 (1944).
7. L. Liebermann, *J. Appl. Phys.* **28**, 205 (1957).
8. B. D. Johnson, R. C. Cooke, W. H. Sutcliffe, *Limnol. Oceanogr.*, in press.
9. B. D. Johnson and R. C. Cooke, *ibid.* **25**, 653 (1980).
10. G. A. Riley, *ibid.* **8**, 372 (1963).
11. D. C. Blanchard and A. H. Woodcock, *Tellus* **9**, 145 (1957).
12. H. Medwin, *J. Geophys. Res.* **75**, 599 (1970).
13. We thank R. M. Gershey for helpful comments. Supported by grants A-7131 and A-8358 from the Natural Sciences and Engineering Research Council of Canada and by grant SRG.21 from NATO.

5 January 1981; revised 20 March 1981

Solar Photovoltaic Power Systems: Will They Reduce Utility Peaking Requirements?

Abstract. *From an analysis of the long-run electric generating requirements of several representative utilities, it is concluded that the energy supplied by solar photovoltaic power devices will displace primarily base-load, and to a lesser extent intermediate, generating plants, even at relatively modest penetrations corresponding to several percent of the utility peak load. Attaching photovoltaic devices to the utility grid will not yield significant fuel oil savings over the long run, in which utilities approach the economic optimum generating mix, and will increase peak plant requirements. Utility capacity and fuel savings of photovoltaic devices are reported both for the case without storage and for the case in which the utility has access to load-leveling storage.*

Solar photovoltaic (PV) power systems, capable of converting incident sunlight directly to electricity, have become the subject of an intensive national research and development effort. Although costs of PV arrays are currently high, there is considerable optimism among researchers that system costs will be reduced significantly over the coming decade. If development efforts are successful, PV devices may one day be capable of generating electricity at costs competitive with conventional utility power.

Given the intermittent nature of solar radiation and the high cost of electric storage, most applications will require addition of an auxiliary power supply to supplement the PV system output and ensure that load is reliably met (*1–3*). Having the electric utility provide this backup power is a major rationale for attaching PV devices to the electric grid. For grid-connected PV systems, available solar power will be either delivered to a local load or exported back to the utility system, in both cases displacing power that would otherwise be supplied by the utility's conventional generating units. Should PV system penetration levels become significant, the aggregate output from the PV devices will cause major changes in the shape and magnitude of the utility load curve and, in the long run, directly affect utility capacity, fuel, and operating requirements.

This report summarizes findings of a recent study that evaluated the long-run

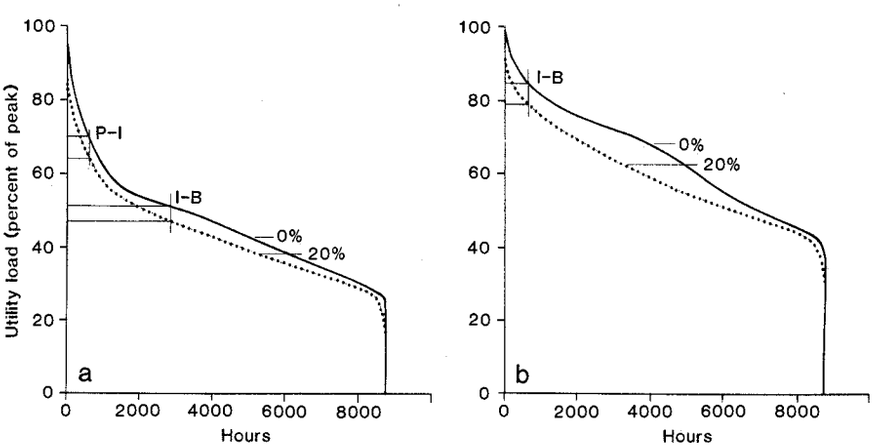

Fig. 1. Annual load duration curves, or cumulative frequency distributions, for 1975 for service areas in the (a) Mid-Atlantic and (b) Southwest regions. Loads are normalized to the maximum no-solar yearly load. Load duration curves are shown for 0 percent solar and for an aggregate (rated) PV capacity equal to 20 percent of the peak utility load. Vertical lines *P-I* and *I-B* refer to the breakpoints between most efficient operation of peak, intermediate, and base-load plants. For the Southwest utility only the breakpoint between coal and oil generation (*I-B*) is shown.

0036-8075/81/0710-0211$00.50/0 Copyright © 1981 AAAS